frontiers in Environmental Science

ORIGINAL RESEARCH
published: 14 March 2022
doi: 10.3389/fenvs.2022.825112

Highly Sensitive Fluorescent Biosensor Based on Acetylcholinesterase and Carbon Dots–Graphene Oxide Quenching Test for Analytical and Commercial Organophosphate Pesticide Detection

Maria I. Gaviria[1], Kaory Barrientos[2], Juan Pablo Arango[2], Juan B. Cano[3] and Gustavo A. Peñuela[1]*

[1]GDCON Research Group, Engineering Faculty, Universidad de Antioquia, Medellín, Colombia, [2]GIBEC Research Group, Life Sciences Faculty, Universidad EIA, Medellín, Colombia, [3]GIMEL Research Group, Engineering Faculty, Universidad de Antioquia, Medellín, Colombia

OPEN ACCESS

Edited by:
Eduardo Torres, Benemérita Universidad Autónoma de Puebla, Mexico

Reviewed by:
Shaohua Chen, South China Agricultural University, China
Lingxin Chen, Yantai Institute of Coastal Zone Research (CAS), China

***Correspondence:**
Maria I. Gaviria
mariai.gaviria@udea.edu.co

Specialty section:
This article was submitted to Water and Wastewater Management, a section of the journal Frontiers in Environmental Science

Received: *30 November 2021*
Accepted: *27 January 2022*
Published: *14 March 2022*

Citation:
Gaviria MI, Barrientos K, Arango JP, Cano JB and Peñuela GA (2022) Highly Sensitive Fluorescent Biosensor Based on Acetylcholinesterase and Carbon Dots–Graphene Oxide Quenching Test for Analytical and Commercial Organophosphate Pesticide Detection. Front. Environ. Sci. 10:825112. doi: 10.3389/fenvs.2022.825112

Chlorpyrifos formulations are the most used in Colombia and other countries for crop protection, and their presence has been proven in many water sources. The application of nanomaterials, including carbon quantum dots (CD), can significantly improve the performance of optical biosensors for quick and accurate detection of these pesticides. In this work, naturally fluorescent and nontoxic CD were conjugated with acetylcholinesterase (AChE) as a bioreceptor, to produce a fluorescent biosensor. This system was modulated with graphene oxide (GO), showing a fluorescence recovery in the presence of the pesticide. The biosensor was evaluated for the detection of pure chlorpyrifos (CPF), profenofos (PF), and a commercial formulation called Lorsban®. A limit of detection (LOD) as low as 0.14 and 2.05 ppb for chlorpyrifos and Lorsban®, respectively, was obtained. Profenofos did not show any recovery with this system at the evaluated concentrations. The system also showed a good selectivity in the presence of proteins (BSA) and other organic substances (Glucose) usually present in drinking water. The specificity was also evaluated against cypermethrin and methomyl commercial formulations showing minimal interference. To the best of our knowledge, this is one of the few works reporting the detection of commercial pesticide formulations with promising results.

Keywords: carbon dots, nanomaterial, fluorescent biosensor, pesticide, chlorpyrifos, enzyme

HIGHLIGHTS

- A biosensor based on acetylcholinesterase and carbon dots for OP detection was developed.
- The biosensor shows ultralow LOD for chlorpyrifos in commercial and analytical grades.
- The biosensor was applied for OP detection without the interference of coexisting substances, even in tap water.

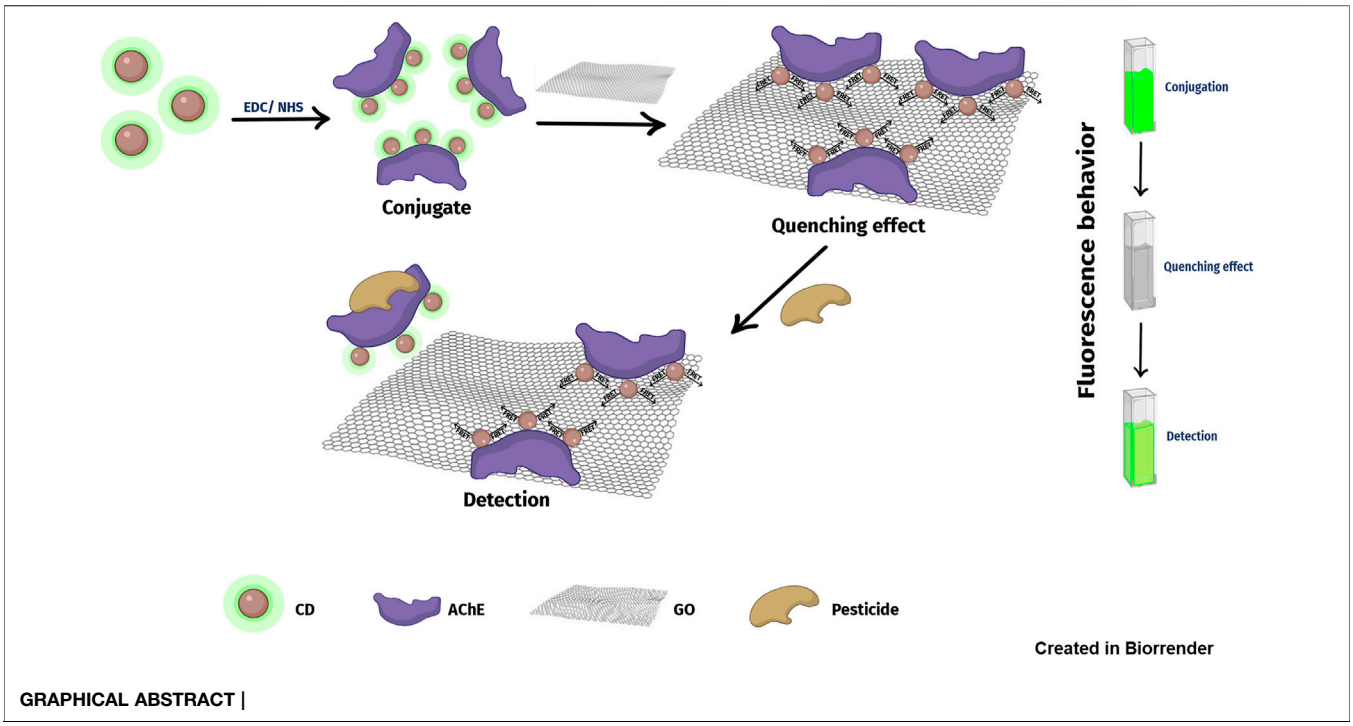

GRAPHICAL ABSTRACT |

INTRODUCTION

The intense use of pesticides has been a common practice for almost 60 years in the agricultural value chain (Vinotha Alex and Mukherjee, 2021). In this way, it is possible to find pesticides with a target in rodents, insects, plants, or microorganisms that can compromise food, wood, or other raw material production. According to the Food and Agriculture Organization (FAO) in 2018, the world consumption of pesticides reached 4 million tons, with Asia at first place followed by the United States and Latin America (FAO, 2018). Humans can get exposed to pesticides in different ways. For instance, farmers in developing countries, like Colombia, are one of the main groups exposed, and also workers of the production and transportation of the pesticide. Furthermore, the public, in general, is exposed through the consumption of food (fruits and vegetables) but usually in lower amounts. Pesticides could be on water sources too, thanks to runoff processes. This exposure to pesticides is related to serious diseases, like non-Hodgkin lymphoma (Luo et al., 2016), Parkinson's disease (Mostafalou and Abdollahi, 2018), as well as respiratory and reproductive disorders (Ramírez and Lacasaña, 2001). Moreover, some pesticides can cause oxidative stress in the cell, leading to cytotoxic and genotoxic effects (Ubaid ur Rahman et al., 2020).

Organophosphate pesticides (OPs) are the most used insecticides worldwide, especially after organochlorine pesticides were prohibited in the 1970s due to their high environmental persistence and toxicity (Sidhu et al., 2019). OP exhibits neurotoxicity because they can block the acetylcholinesterase enzyme (AChE) irreversibly (Vinotha Alex and Mukherjee, 2021). That blockage causes the accumulation of acetylcholine (ACh), a key neurotransmitter for the synaptic process in the neuro-muscular interface (Sidhu et al., 2019). Specifically, the effects of ACh accumulation are the hyperstimulation of muscarinic and nicotinic receptors (Jokanović, 2018), with intoxication symptoms, such as sweating, miosis, and diarrhea. OP acute exposure can cause death, while chronic exposure causes nervous, reproductive, and respiratory effects even more than 30 years after exposure (King and Aaron, 2015). Among the OPs, chlorpyrifos (CPF) is the main active principle used in a wide range of crops, and it has a relatively low persistence and low toxicity. However, CPF and CPF-oxon, as common bioactive products, block AChE (Ubaid ur Rahman et al., 2020). EPA recently banned CPF (august 2021), so it is still being used in developing countries under the commercial names of Lorsban, Dursban, Equity, Suscon, Empire20, and Whitmire PT270. On the other hand, Profenofos (PF) is an OP that is widely used in agriculture. The presence of PF in the biological system has gained importance due to bioaccumulation in the food chain (Mishra et al., 2015).

For OP detection, robust techniques are used, such as chromatography (HPLC, HPTLC, LC/MS, GC/μECD, and GC/MS), spectrophotometry, and FT-Raman spectroscopy (Talari et al., 2021). These methods require pretreatment of samples from natural sources, such as rivers, which means that analysis times are not very short, and there is an increase in their cost (Campuzano et al., 2019). In this context, biosensors have become promising tools for rapid and effective OP detection. The interest in biosensors for OP detection is a growing research area because of their ease in handling, the low-cost potential of their components, and the possibility of real-time quantification (Gaviria-Arroyave et al., 2020).

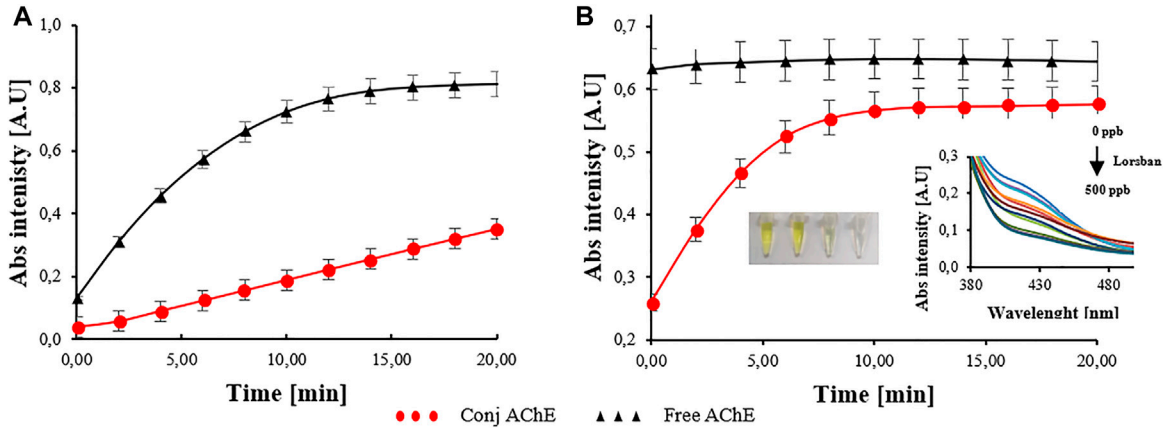

FIGURE 1 | Kinetic curves of the free and conjugated enzyme at different concentrations. **(A)** Acetylcholinesterase (AChE) at 1 U mL^{-1} and **(B)** AChE at 5 U mL^{-1}. The inset in **(B)** shows the linear inhibition of the free AChE at 5 U mL^{-1} with increasing concentrations of Lorsban (0, 50, 100, 150, 200, 250, 300, 350, 400, 450 years 500 ppb). n = 4 independent experiments.

Biosensors can act as alarms when the water enters the water treatment plants for human consumption with a pesticide. Once the alarm is made, the presence of the pesticide can be confirmed with chromatographic techniques.

In recent years, optical biosensors based on nanomaterials have been developed with lower detection limits and greater stability. The application of nanomaterials, including carbon dots (CDs), can significantly improve the performance of the systems. CDs are zero-dimension quasi-spherical nanoparticles, composed primarily of carbon and oxygen, usually with sizes below 10 nm (Abdul et al., 2019; Campuzano et al., 2019). CDs have gained a lot of attention because they have optoelectronic properties, such as quantum dots, especially when it comes to fluorescence. CDs, unlike quantum dots, have excellent biocompatibility (Liu et al., 2019).

To promote the real application of biosensors, their sensitivity and specificity must be improved, and their performance tested in conditions close to fieldwork. In this work, we investigate how CDs can significantly improve the performance of optical biosensors. We developed a biosensor to detect chlorpyrifos and profenofos in water. The system is based on AChE as a biomediator, CD acting as a fluorescent transductor, and graphene oxide (GO) as a quenching agent. The CDs were synthesized by our laboratory in previous works (Barrientos et al., 2021) from African-oil palm biochar. The biosensor was evaluated under different concentrations of pure pesticides (chlorpyrifos and profenofos) and commercial pesticides (Lorsban®), obtaining a limit of detection (LOD) as low as 0.14 and 2.05 ppb for chlorpyrifos and Lorsban®, respectively. Profenofos did not show any recovery with this system at the evaluated concentrations. The system also shows a good selectivity against proteins (BSA) and other organic substances (glucose) usually present in drinking water, even in tests with tap water. The specificity was also evaluated against two types of pesticides: cypermethrin (pyrethroid type) and methomyl (carbamate type), showing expected behavior with a slight system response with cypermethrin and a marked response with methomyl. To the best of our knowledge, it is one of the few works where the performance of the system is tested against residues of the commercial formulation and not only using pure pesticides. The positive results allow progress in the integration of nanomaterials in the development of biosensors, as well as advance in the commercial projection of these systems to protect the health of rural communities.

EXPERIMENTAL SECTION

Chemical Used

All chemicals were of analytical grade. Acetone and acetonitrile were bought from PanReac AppliChem® and used as received. Commercial solutions of chlorpyrifos (Lorsban®), methomyl (Lannate® 40), and cypermethrin (Invetrina® 200 EC) were bought from a local distributor, and dilutions were made using double deionized water. For conjugation steps, EDC (1-ethyl-3-[3-dimethylaminopropyl]carbodiimide), NHS (N-hydroxysuccinimide), and 2-mercaptoethanol (ME) were bought from Thermo Fisher. Single-layered graphene oxide (GO) was purchased from ACS material. Analytical standards of chlorpyrifos (CPF) and profenofos (PF), as well as acetylcholinesterase (AChE) from *Electrophorus electricus*, acetylthiocholine (ACTh), and DTNB [5,5′-dithio-bis-(2-nitrobenzoic acid)], were bought from Merck. All tests were carried out in triplicate. Carbon dots (CDs) were synthesized from African-oil palm biochar (*Elaeis guineensis*) according to our previous work (Barrientos et al., 2021). Double deionized water was used through all the experiments (Milli-Q ultrapure water system with a 0.22-μm filter, Merck Millipore).

Conjugation Procedure

The covalent conjugation technique was used, through carbodiimide chemistry following the protocol described by

ThermoFisher scientific.[1] EDC was used in the presence of NHS, to obtain an amide bond between carboxylic acids from the CD and primary amines present in the AChE. Briefly, 500 ppm of CD water solution was put in contact with 0.05 M of EDC and 0.1 M of NHS and letting them react for 15 min. Then ME (0.5 M final concentration) was added to stop the activation of the carboxylic groups, followed by 2-h dialysis (3.5 kDa, four water changes). Before the addition of the AChE, the pH was adjusted to 7.45 with sodium bicarbonate. An appropriate amount of AChE (final concentration of 5 U mL^{-1}) was added and left for the reaction for 2 h. Finally, the remaining carboxylic active sites of the CDs were blocked to prevent nonspecific detection. For that, ethanolamine (20 mM final concentration) in phosphate buffer pH 7.45 was added, followed by 30 min of dialysis (3.5 kDa, two water changes). The AChE–CD conjugates were stored under 4°C until detection assays and remained active for at least 1 week.

Enzymatic Activity

The enzymatic activity of the free and conjugated enzyme was evaluated following the protocol described by Ellman et al. (1961). In typical free AChE activity evaluation, 25 µl of DTNB (0.01 M), 25 µl of ACTh (2 mM), and 10 µl of AChE with different activities were mixed with 40 µl of phosphate buffer (0.1 M, pH 8). For the conjugated AChE the same reaction mixture was used, but 50 µl of the sample was added instead of pure AChE and phosphate buffer. The solutions were mixed completely, and the formation of 2-nitro-5-thiobenzoic acid (TNB) as reaction product (416 nm) was monitored at 37°C for 20 min to determine the enzymatic activity. For preliminary Lorsban® evaluation, 25 µl of the pesticide at different concentrations was mixed with 25 µl of AChE (100 U µl ml^{-1}) and subsequently incubated at 37°C for 30 min. Then 50 µl of ACTh (5 mM) and 50 µl of phosphate buffer (0.1 M, pH 8) were added, and the mixture was incubated again at 37°C for 25 min. Finally, 150 µl of DTNB and 200 µl of Mili Q water were added and vigorously mixed for 5 min. Absorbance spectra were taken between 300 and 800 nm, and the peak for TNB formation (416 nm) was monitored.

Characterization Techniques

UV-Vis and fluorescence measurements (spectrum and punctual) were done in a Varioskan Lux (Thermo scientific, SkanIt Software 4.1) on 200 µl working volume microplates (Falcon™ nontreated black 96-well) at 25°C with 1-nm optical step. The stability of the AChE–CD conjugates were investigated through Z potential techniques on a Nanoplus-3. The measurement was performed using 0.2-µm filtered solutions in a DTS1070 cell, with water as a dispersant (refractive index: 1.330). The shape and size of the AChE–CD conjugates were taken using high-resolution transmission electronical microscopy (HR-TEM) on an FEI-Tecnai F20 Super Twin TMP.

[1]https://www.thermofisher.com/order/catalog/product/24500?SID=srch-srp-24500

Pesticide Detection

Chlorpyrifos and Lorsban® were evaluated in a range between 0 and 0.1 ppm, while profenofos was evaluated between 0 and 10 ppm. For this purpose, different dilutions were made in Milli-Q water. For the detection assay, 890 µl of the conjugate and 10 µl of graphene oxide (100 ppm GO final concentration) were vigorously mixed in different vials. After 15 min, 100 µl of the appropriate dilution of the pesticide was added to reach a desired final concentration. The solution was vigorously mixed and made to sit for another 15 min until fluorescence recovery analysis. The amount of the pesticide dilution was replaced by Milli-Q water for the control.

The relativity fluorescence recoveries of CD at emission and excitation wavelengths of 420 and 320 nm, respectively, against increasing concentration of the evaluated pesticides were plotted. Higher concentrations of chlorpyrifos, profenofos, and Lorsban® cause higher fluorescence recovery. The limits of detection (LOD) and quantification (LOQ) of the system were calculated based on the parameters of the analytical curve in the linear range (from the semilog plot), using the following equations adapted from Khoris et al. (2021):

$$LOD \leq e^{\frac{F_0+3.3\sigma-c}{s}} \quad (1)$$

$$LOQ \leq e^{\frac{F_0+10\sigma-c}{s}} \quad (2)$$

with F_0 σ, c, and s as the fluorescence signal of the blank, the standard deviations of the blank, the y-intercept, and the slope of the calibration curve, respectively.

All experiments were treated and analyzed in triplicate. For LOD calculations, a one-way ANOVA was performed using R-studio software, and $p \leq 0.05$ was considered as statistically significant.

RESULTS AND DISCUSSION

Conjugate Characterization

CDs were synthesized from African-oil palm (*Elais guinensis*) and characterized in our previous work (Barrientos et al., 2021). The CDs have plenty of carboxylic groups, and they had a maximum emission peak at λ = 420 nm under excitation of λ = 320 nm. The CD showed a brownish-yellow color under daylight and blue emission under ultraviolet light (insert in **Figure 3A**). They were stable in an aqueous solution for several weeks without losing their optical properties. **Figure 1** shows the kinetic curves for the activity of the conjugate of CD and AChE, at two enzymatic concentrations (1 and 5 U mL^{-1}) and a fixed concentration of the substrate ACTh of 0.5 mM. Based on literature review and previous works done by our research group (Catalina Rodríguez et al., 2013; Betancur et al., 2018), preliminary assays with free AChE between 1 and 5 U mL^{-1} and ACTh between 0.25 and 0.75 mM were done to optimize enzymatic and substrate expenditure. AChE concentration was the only significant factor (p-value <0.001, n = 4). We found that even though for the free enzyme the maximum activity is obtained for the concentration of 1 U mL^{-1} (data not shown), in the case of the conjugate, the best performance is obtained at 5 U mL^{-1} with a

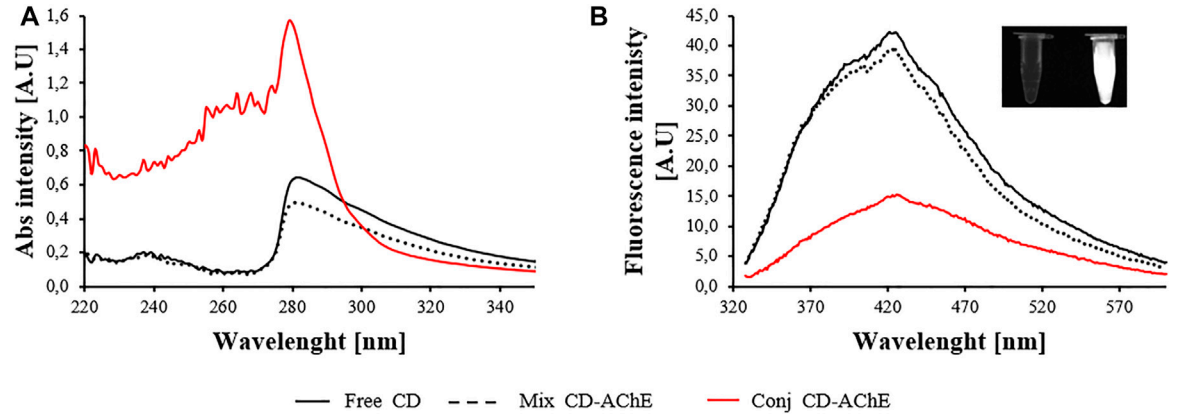

FIGURE 2 | (A) UV-Vis spectrum showing the increase in the peak at 280 nm for the conjugated carbon dot (CD) and AChE at 5 U mL^{-1}, due to amide bond formation. **(B)** Fluorescence emission spectrum (excitation at 320 nm) showing the decreasing fluorescence of the CD for the conjugation of CD and AChE at 5 U mL^{-1}. The inset in **(B)** shows the CD under UV light and the mili Q water control.

Vmax of 35.88 versus 15.14 μmol ml^{-1} min^{-1}. Additionally, the conjugate at 5 U mL^{-1} retains 87% of the activity compared with the free enzyme. This phenomenon can be explained by the enzyme–substrate affinity constant evaluated for the free enzyme, since when the CDs are conjugated with AChE, it is possible that the active site is affected, or its environment is modified reducing the affinity of acetylcholine at lower amounts of enzyme. Furthermore, some authors report the inhibition of AChE activity by some CDs, especially those with antioxidant properties (Suner et al., 2021). The insert in **Figure 1B** shows the decreasing absorbance intensity at 416 nm, indicating a lineal inhibition of the free AChE at 5 U mL^{-1} in the presence of Lorsban® for a range between 0 and 500 ppb. This range of concentrations suggests a good approach for the evaluation of the biosensor. For further assays, a fixed enzyme and substrate concentration of 5 U mL^{-1} and 0.5 mM were used, respectively.

To verify the conjugation between CD and AChE (amide bond formation), the UV-Vis and fluorescence emission spectrum for the free CD, mixed CD and AChE, and conjugated CD with AChE are shown in **Figure 2**. The CDs have an absorption peak at 280 nm possibly attributable to n-π* transition of C=O bonds (Zheng et al., 2015), as does the unconjugated mixture of CD and AChE. In the same graph, we can see that the conjugated mixture of CD and AChE presents a higher peak at the same wavelength, due to the absorption of the amide bond whose presence has increased due to conjugation (Song and Zhang, 2019). The formation of an apparent new peak at 260 nm associated with the conjugation process is also observed, although the signal is noisy (Sharma et al., 2019). Regarding the fluorescence spectrum, for all the samples, a maximum emission peak was obtained at 420 with 320 nm as excitation value. We can see in the fluorescence spectrum (**Figure 2**) how the conjugated mixture decreases the original fluorescence of the CD. This is due to the modification of the surface chemical groups in the CD; this mechanism is directly responsible for the fluorescence (Liu et al., 2019).

The stability and morphology of the conjugate were verified with HR-TEM and Z potential. **Figure 3B** represents a TEM image of AChE-conjugated carbon dots at a concentration of 5 U mL^{-1} and 500 ppm, respectively. In a previous work (Barrientos et al., 2021), the HR-TEM was utilized to investigate the morphology and average size of the carbon dots derived from *Elaeis guineensis*. In that study, we obtained nanoparticles mono-dispersed with an average size of 2.5 ± 0.7 nm, which are close to the average size obtained in this work of 3.7 ± 0.5 nm as seen in the histogram of particle diameter distribution of carbon dots (**Figure 3D**). Besides, **Figure 3B** reveals particles with a nearly spherical shape and an average diameter of 16.± 3.93, which is comparable with the dimensions reported for the acetylcholinesterase tetramer from *Electrophorus electricus* (Raves et al., 1998; Bourne et al., 1999), and TEM images obtained from the enzyme to study its location in the cell (Dobbertin et al., 2009; Blotnick-Rubin and Anglister, 2018). The AChE particles are surrounded by carbon dots, which could be given by the union of the carboxylic acids present on the surface of the carbon dots (Barrientos et al., 2021) with the amines of lysine (272) and arginine (1,560) residues available on the surface of the enzyme (**Figure 3E**). Because of similarities in size, shape, and availability of amines, the TEM images suggest that conjugation of carbon dots with the AChE enzyme has been given because of our conjugation protocol.

Furthermore, the HR-TEM images in **Figures 3B, C** reveal the change in the aggregation morphology of the CD for the conjugate with AChE and the conjugate in the presence of GO. We found that particles of AChE are surrounded by a lot of CDs, forming aggregates. This aggregation could explain the decrease in the fluorescence intensity for the conjugate compared with the bare CDs, as shown in the inset. For the conjugate in the presence of GO, the aggregation is stronger in the TEM images and even with the naked eye. As can be expected, the decreasing fluorescence intensity of the conjugate is almost complete in the presence of GO

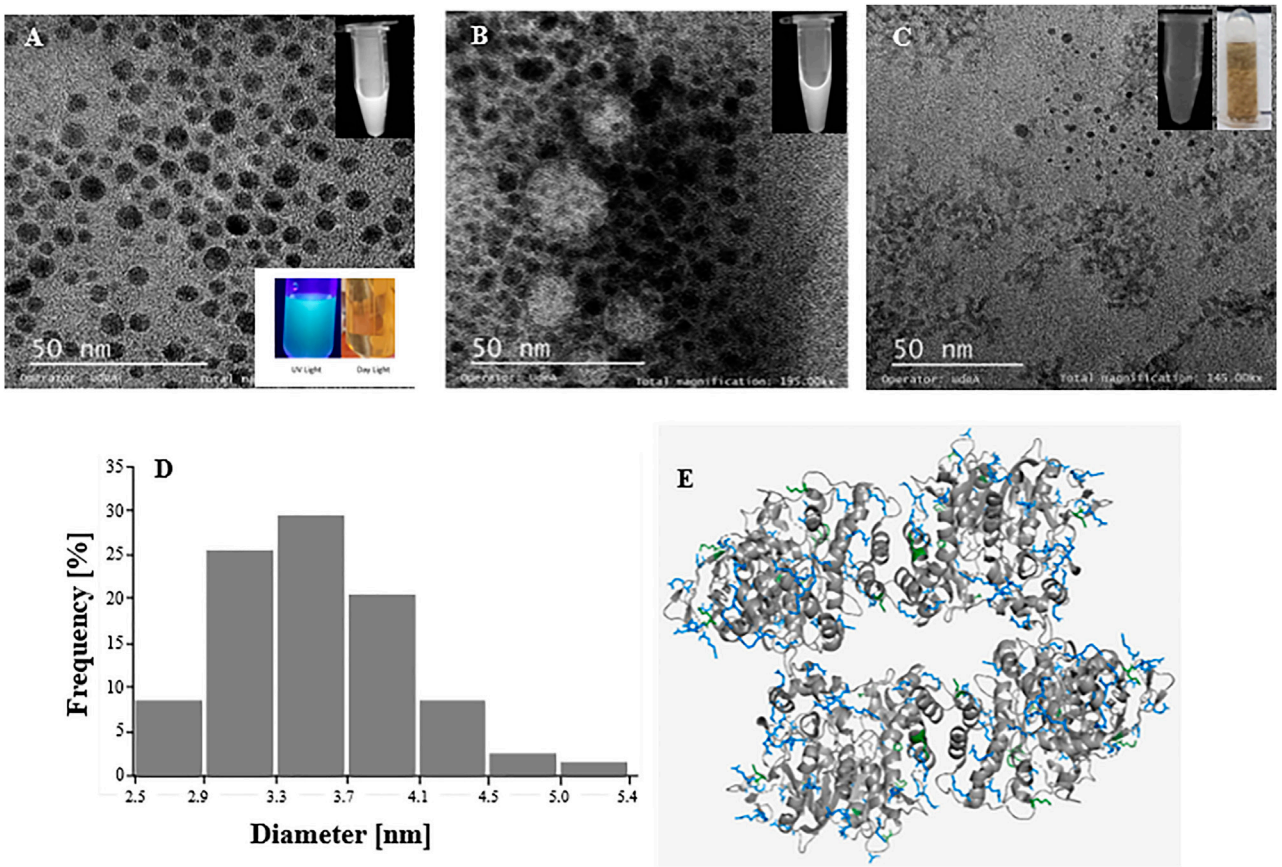

FIGURE 3 | High-resolution transmission electronical microscopyHR-TEM) images for **(A)** CD, **(B)** CD conjugated with AChE at 5 U mL^{-1} and **(C)** CD–AChE conjugate and graphene oxide (GO) at 100 ppm. **(D)** CD histogram and **(E)** ribbon model of the AChE enzyme structure (PDB ID 1C2O) and representation of amino acids lysine (green) and arginine (blue). The insets in **(A–C)** show the changes in the fluorescence intensity under UV light. The inset in **(C)** also shows the aggregation of the conjugate in the presence of GO at 100 ppm as the main mechanism for CD fluorescence quenching.

(100 ppm), and the mechanism of quenching is discussed in the next section.

The Z potential is an indicator of conjugate stability since it is a measure of the charge repulsion or attraction between the particles from their surface to the boundary of the diffuse layer (Shukla and Iravani, 2019). The measurements afford a value of −51.27 mV, indicating that besides the big size and broad distribution of populations, the conjugate particles have great stability. This finding also supports that the aggregation of the conjugate in the presence of GO is not related to the stability of the conjugate itself but the interactions of the chemical groups in both molecules.

Finally, the storage stability of the CD–AChE conjugate was verified (**Figure 4**). Fresh conjugate was stored at 4°C for 30 days, and the fluorescence signal was monitored. The fluorescence intensity of the conjugate at 16 days shows an increase, probably due to the disintegration of the amide bond between the CD and the AChE or the decay of weak interactions between particles, so that the CD regains some of their initial fluorescence. However, at 24 days, the fluorescence of the CD decay is almost at the initial value, reaching a minimum value of 43% at 30 days. This effect could be explained since the CD alone in solution has shown great stability, but the interactions with the residuals of the enzyme and the by-products of the synthesis and conjugation processes are unknown. The CD after 30 days could be aggregated, losing their fluorescence. Furthermore, the poor

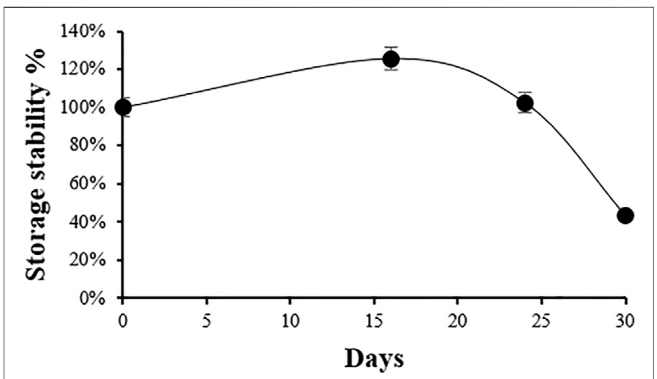

FIGURE 4 | Percentage of storage stability at 4°C for the CD–AChE conjugate showing the retention of 43% of initial activity within 30 days.

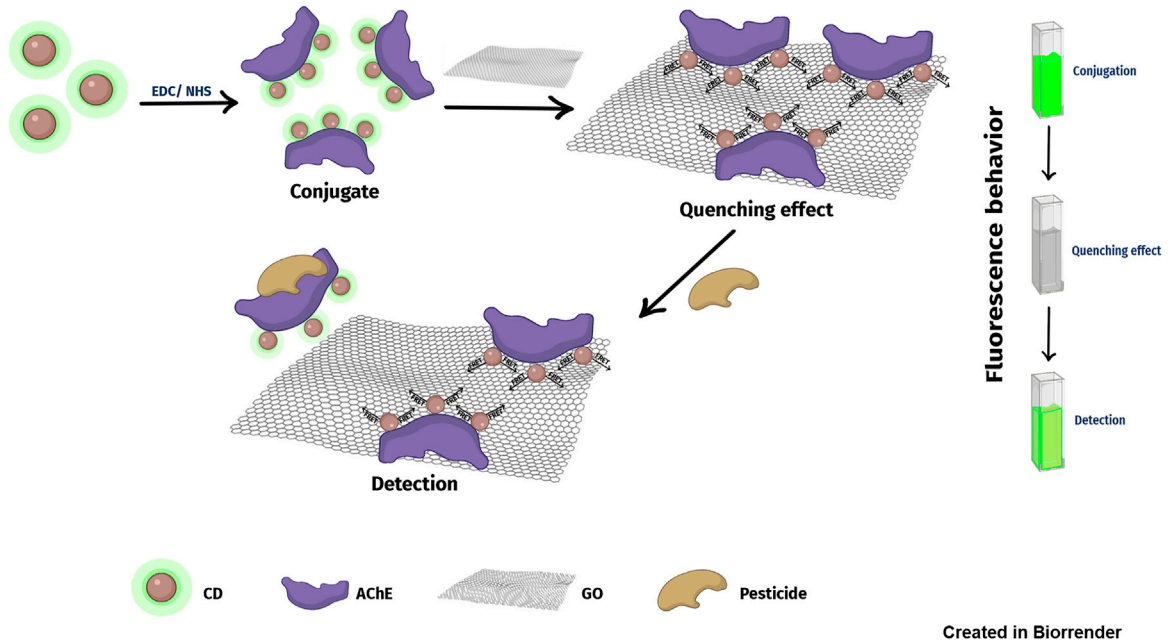

FIGURE 5 | The detection mechanism of the proposed biosensor showing the quenching of the fluorescence for the CD conjugated with AChE in the presence of GO, and the recovery of the fluorescence signal in the presence of the pesticide.

stability of enzymes at physiological pH and under temperature changes is reported (Ramnani et al., 2016). Some authors advise improving the stability through immobilization, reaching up to 70% of initial activity within 30 days for electrochemical systems (Zhang et al., 2021).

Pesticide Detection Mechanism

The detection mechanism of the proposed sensor is shown in **Figure 5**. CDs are covalently bonded to AChE causing a decrease in the fluorescence intensity as we previously described in HR-TEM images (**Figure 3**). Then we added an optimized GO concentration of 100 ppm, reducing to 57% the initial fluorescence, and indicating the quenching phenomena in a turned-off system. GO is a flat sheet of carbon atoms one atom thick, which are linked by sp^2 hybridization (Gaviria-Arroyave et al., 2020). Since CDs are biochar derived through a carbonization method, it is possible that they present the same hexatomic ring of atoms as GO, causing π–π spontaneous interactions promoting fluorescence quenching (Zheng et al., 2015).

Aromatic residues in the AChE and cyclic groups in the CD interact with sp^2 hybridization groups in the GO, bringing the former closer to the CD so that the quenching is probably generated through the FRET principle. When the pesticide molecules are present, the molecules interact with the enzyme due to their affinity and the ability of the organophosphorus pesticides to irreversibly inhibit the AChE (Berger and Schaumburg, 2005; Chen and Cashman, 2013; Ratner and Jabre, 2016). Consequently, the enzyme will undergo conformational changes (Pang et al., 2009; Colovic et al., 2013; Sánchez-Santed et al., 2016; Cacciotti et al., 2020) leading to a CD/AChE/pesticide complex. Therefore, the π–π interactions between the complex and the GO are weakened because the groups involved are shielded, a behavior seen in the interaction between CD complex with GO (Chang et al., 2010; He et al., 2010; Li et al., 2013). As a result, the CDs are detached from the GO, leading to emission of fluorescence by the conjugate complex in the presence of the pesticide. GO, as well as other carbonaceous nanomaterials, have a high surface-to-volume ratio, highly distance-dependent fluorescence quenching ability (Bai et al., 2020), and high energy/electron transfer capability, which make it a universal quenching agent for the development of FRET-based biosensors (Lee et al., 2020). However, to the best of our knowledge, a few studies report the use of GO and AChE in optical systems for pesticide detection. Most of the studies reported GO and AChE in electrochemical sensors, thanks to the stabilization and insulation properties of GO in such systems (Dong et al., 2013; da Silva et al., 2018; Bao et al., 2019; Shamagsumova et al., 2021). Other studies reported the use of CD alone for direct pesticide detection in turning-off systems (Alvandi et al., 2021) and based on the FRET mechanism with the analyte (Ashrafi Tafreshi et al., 2020). Recently, there are some studies reporting biosensors based on CD–AChE conjugates for pesticide detection (inner filter effect—IFE and FRET mechanisms), using different quenching agents, such as Cu^{2+} ions (Reshma et al., 2019), (Xu et al., 2019), 2,3-diaminophenazine (DAP) (Huang et al., 2019), dopamine (Li et al., 2020), and gold nanoclusters (Suo et al., 2020).

CD applications in fluorescence biosensing could be through different mechanisms, such as static quenching, dynamic quenching, photo-induced electron transfer, FRET, and IFE. For the FRET mechanism to occur, characteristics such as the

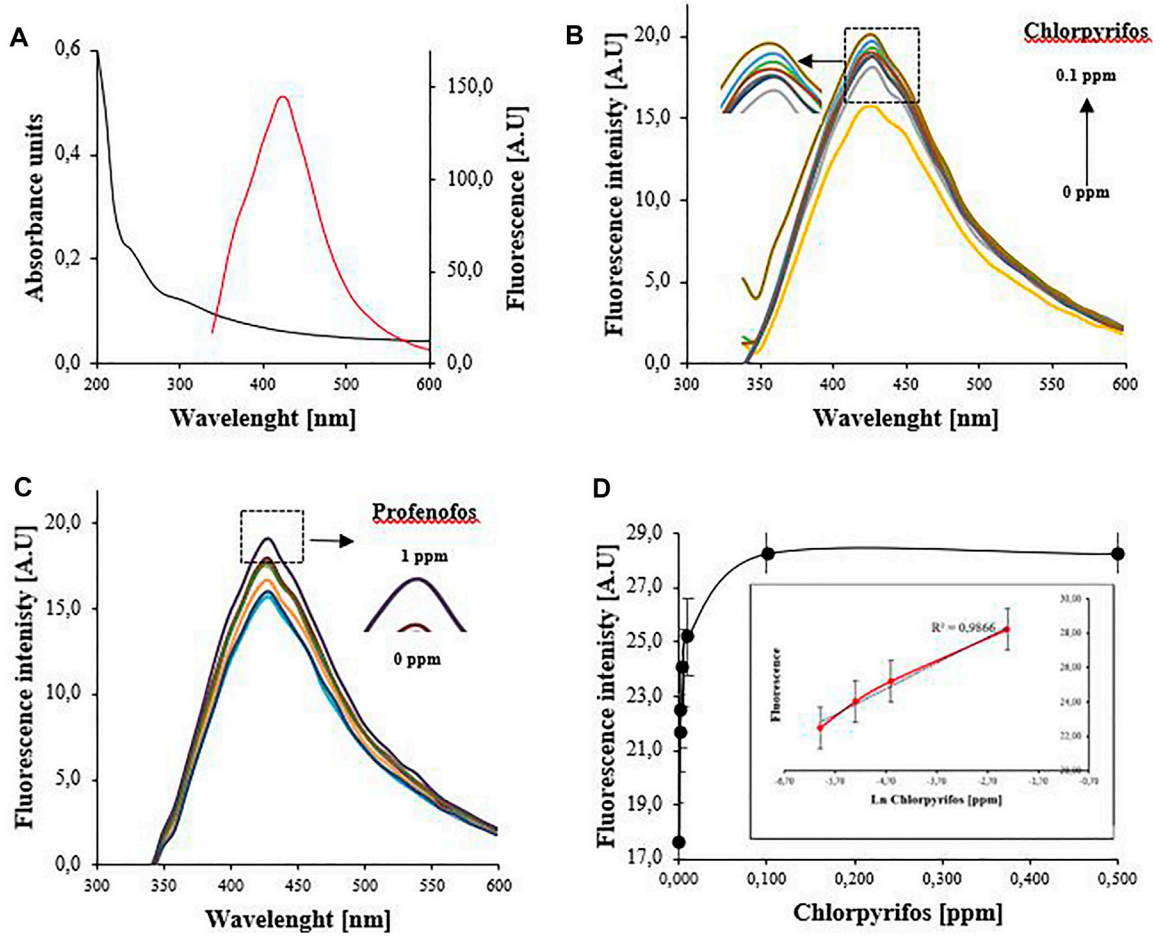

FIGURE 6 | (A) UV-Vis absorbance spectrum of the GO showing a partial overlapping with CD emission spectra at 320 nm (excitation wavelength). Emission spectra for **(B)** chlorpyrifos between 0 and 0.1 ppm and **(C)** profenofos between 0 and 1 ppm. **(D)** Exponential relationship between the fluorescence intensity (λem = 420 nm) and the concentration of chlorpyrifos. Inset: Linear relationship between the fluorescence intensity (λem = 420 nm) and the natural logarithmic value of chlorpyrifos concentration. Profenofos only shows detection at 1 ppm and does not show linear behavior in any range.

overlapping of the emission spectra of the energy donor (CD) with the absorption of the quencher (GO), and the distance between both species within 10 nm must be met (Pirsaheb et al., 2019). Other important aspects are the stability of the donor's fluorescence emission and the high absorptivity of the quencher. As we can see in **Figure 6A**, the absorption spectrum of GO covers a broad range of wavelengths (approximately 240–700 nm), partially overlapping the fluorescence spectrum of CD and making possible the quenching phenomena through the FRET principle, which has been widely reported in the literature (Arvand and Mirroshandel, 2019; Pirsaheb et al., 2019; Zhou et al., 2020). Additionally, biomolecules, such as enzymes and single-stranded nucleic acids, can interact with the GO through π–π stacking or hydrogen bonding, decreasing the distance and facilitating FRET (Lee et al., 2020). Furthermore, it has been sufficiently reported in the literature that optical biosensors based on CDs conjugated with other biomolecules, and GO acting as a quencher for the detection of different analytes, used FRET as the mechanism of detection (Ding et al., 2015; Cheng et al., 2018; Zhou et al., 2020). GO is rich in functional groups, such as carboxyl, hydroxyl, epoxy, etc. These groups are present both on the basal plane and edges leading to a heterogeneous electronic structure with the best probability of interaction with the analyte and, thus, giving more sensible systems (Neema et al., 2020).

Chlorpyrifos and Profenofos Detection

To verify the ability and sensibility of the system to detect pesticides, different concentrations of CPF (0–0.1 ppm) and PF (0–1 ppm) were analyzed. For CPF detection, **Figure 6B** shows the rise in the fluorescence response with the increasing concentration of the pesticide. Also, **Figure 6D** displays the good exponential correspondence between fluorescence intensity and CPF concentration. This is consistent with the detection mechanism previously explained, that is, the more CPF is in the system, the more CD–AChE complex is detached from GO sheets increasing the distance and making FRET impossible, causing the fluorescence recovery of the CD. Furthermore, the fluorescence

TABLE 1 | Comparison of the present method with other reported highly sensitive electrochemical and fluorescence methods based on AChE and nanomaterials for organophosphate pesticide (OP) detection.

Detection method	Nanomaterial	Electrode	Analyte	LOD[a]	Linear range[a]	Ref
Electrochemical	Titanium oxide nanorods (TiO_2-NRs) and reduced graphene oxide (rGO)	GCE	Dichlorvos	2.23×10^{-9} M	2.26×10^{-9} M to 5.65×10^{-8} M	Zhang et al. (2021)
Electrochemical	Semiconducting single-walled carbon nanotubes (s-SWCNTs)	GCE	Methyl parathion	3.75×10^{-11} M	1×10^{-10}M to 5×10^{-6} M	Kumar and Sundramoorthy, (2019)
Photo-electrochemical	Magnetic nanocrystal clusters	mGCE	Chlorpyrifos	3.75×10^{-10} M	2.85×10^{-9} M to 2.85×10^{-6} M	Mao et al. (2017)
Electrochemical	Zinc based metal–organic framework (MOF)	Gold microelectrodes	Chlorpyrifos	1.7×10^{-11} M	2.85×10^{-11} M to 2.85×10^{-10} M	Nagabooshanam et al. (2019)
Detection method	**Fluorescent material**	**Quencher**	**Analyte**	**LOD**	**Linear range**	**Ref**
Fluorescence	Quantum dots (QD)	H_2O_2 production	Malaoxon, paraoxon, dibrom, and dichlorvos	5×10^{-8} M	5×10^{-9} M to 1×10^{-9} M	Wei et al. (2017)
Fluorescence	Aggregation-induced emission fluorogens (BSPOTPE)	SiO_2–MnO_2	Paraoxon	3.6×10^{-9} M	3.6×10^{-9} M to 3.6×10^{-7} M	Wu et al. (2019)
Fluorescence	CD	Au nanoclusters	Diazinon	2.7×10^{-9} M	-	Suo et al. (2020)
Fluorescence	CD	$Cu2^+$	Paraoxon Chlorpyrifos	7.6×10^{-9} M 1.3×10^{-12} M	-	Reshma et al. (2019)
Fluorescence	N-doped CD	Au NPs	Carbaryl	2.9×10^{-10} M	9.9×10^{-10} M to 7.4×10^{-7}M	Chen et al. (2020)
Fluorescence	CD	GO	Chlorpyrifos	$4.1 \times 10–^{10}$ M	7.1×10^{-9} to $2.85 \times 10–^{7}$ M	This work
			Lorsban[a]	$5.8 \times 10–^{9}$ M	$2.8 \times 10–^{9}$ M to $7.1 \times 10–^{8}$ M	

[a]*Note. LOD and linear range are expressed in molarity concerning the molecular weight of chlorpyrifos.*

intensity shows a good linear correlation with the natural logarithm of CPF concentration in the range of 2.5 ppb to 0.1 ppm (7.1–285.2 nM). The linear regression equation for this range ($R^2 = 0.9866$, $^{***}p < 0.001$) was F = 31.842 + 1.5059 ln C, where F and C are the fluorescence intensity and CPF concentration, respectively. The LOD was determined as low as 0.14 ppb (0.41 nM) with an LOQ of 1.4 ppb (3.99 nM).

Despite the good results for CPF detection, the system seems to be less sensitive to PF, since the recovery of the fluorescence was obtained just for the higher concentration evaluated (1 ppm) as is shown in **Figure 6C**. Concentrations below 1 ppm did not cause fluorescence recovery and, in fact, decreased the signal. These results could be explained because CPF is known to be a more potent inhibitor of AChE than other OP, such as monocrotos, acephate, and profenofos (Das et al., 2006). Furthermore, PF is a less recalcitrant pollutant since its DT50 (semidegradation rate) is just 8 days compared with 30 days for CPF (Ismail and Ngan, 2005). No linear range, LOD, or LOQ were found for PF.

Performance comparison of different highly sensitive electrochemical and fluorescence methods based on AChE and nanomaterials for OP detection are shown in **Table 1**. The LOD of this work is lower than those of other methods based on simple strategies and nanomaterials. This work uses a nondoped CD and a simple well-established quencher (GO), obtaining a sensitive LOD with a simple and reproducible methodology. Furthermore, the wider linear range shows the viability of the system for real-world applications. Other reported methods with ultralow LOD and wider linear ranges are based on more sophisticated strategies like using metal–organic frameworks (MOF), doped CDs, or a combination of multiple nanomaterials; in these methods, the sensibility is improved but practical applications could be difficult.

Detection of Commercial Chlorpyrifos (Lorsban®)

The response of the system in the presence of different concentrations (0–0.1 ppm) of Lorsban as a commercial OP model was evaluated. Lorsban is a milky white color, an emulsion in water formulation that contains 40.2% of chlorpyrifos as a main active principle and other nondeclared ingredients, such as coadjutants. These ingredients could be solvents, humectants, thickeners, and surfactants, among others. The coadjutants are needed to allow practical application of the active compound (water dilution) and increase its performance (better penetration and stability). However, these ingredients could interfere in the detection of chlorpyrifos as an active compound in real-world applications, and the verification of the analytical parameters between pure compound and commercial formulation should be done. **Figure 7A** shows the increase in the fluorescence signal with increasing concentration of Lorsban, and **Figure 7B** shows the

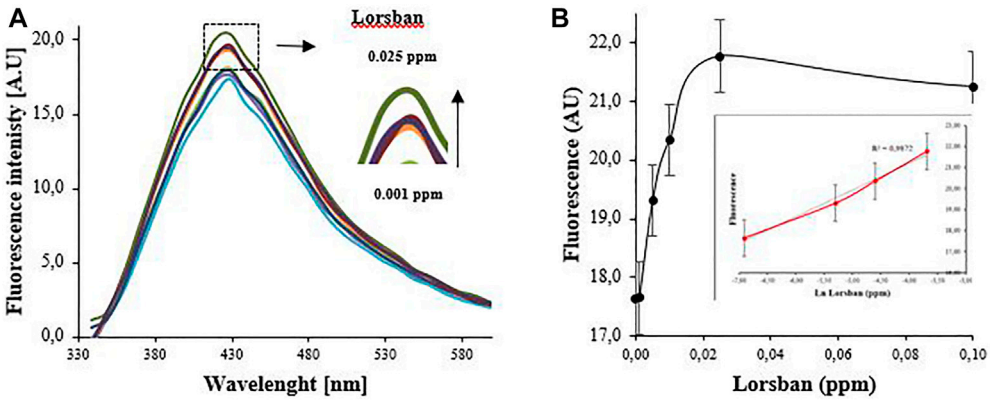

FIGURE 7 | (A) Lorsban between 0 and 0.1 ppm. **(B)** Exponential relationship between the Fluorescence intensity (λem = 420 nm) and the concentration of Lorsban. Inset: linear relationship between the fluorescence intensity (λem = 420 nm) and the natural logarithmic value of Lorsban concentration.

exponential relationship between fluorescence intensity and Lorsban concentration. As was expected, the performance of the system for Lorsban seems to be less sensitive than pure chlorpyrifos detection, with an LOD of 2.05 ppb (5.84 nM) and a narrow linear range between 1 and 25 ppb (2.8–71 nM). The linear regression equation for this range (R^2 = 0.9872, $^{**}p <$ 0.01) was F = 26.1470 + 1.2401 ln C, where F and C are the fluorescence intensity and Lorsban concentration, respectively. These results confirm that other substances present in the formulation reduce the sensibility of the sensor. The mechanism could be explained through the shielding effect of some ions over the conjugate and the steric effect of the substances, neither reducing the possibility of the conjugate CD–AChE to interact with the active principle or the ability of the conjugate to detach from the GO in the presence of less amount of compound. Furthermore, the loss of enzymatic activity under pH variations is well known (Işık, 2020), and the pH value for Lorsban solutions in the evaluated range of concentrations increases above the optimal reported value for AChE activity (7.5) reaching 8 and suggesting a potential step in pH sample adjustment for field implementation. However, the system is still sensible enough for the detection of Lorsban residues, and the good LOD combined with the simplicity of the system suggests its implementation potentially reducing the steps of field sample processing before evaluation. As far as we know, works on biosensors reporting commercial OP detection are very scarce, so the present results contribute to the state of the art.

Selectivity and Matrix Effect of the System

To evaluate the selectivity of the system, different substances commonly found in water sources and two non-organophosphate commercial pesticides were selected. Briefly, 0.1 ppm of glucose, bovine serum albumin (BSA), Lannate® (methomyl, carbamate type), and Invetrina® (cypermethrin, pyrethroid type) were tested individually with the system using tap water and compared with 0.01 ppm of CPF. As shown in **Figure 8A**, the system did not respond to the presence of glucose, BSA, or Lannate® as the model carbamate pesticide. This behavior is interesting since it is known that AChE is inhibited by carbamate pesticides (Kaur and Prabhakar, 2017), but in this study, the combination of nanomaterials like CD and GO could have a protective effect increasing the specificity of the system (Vinotha Alex and Mukherjee, 2021). Additionally, OP covalently phosphorylates AChE's serine residues, causing a nonreversible strong inhibition

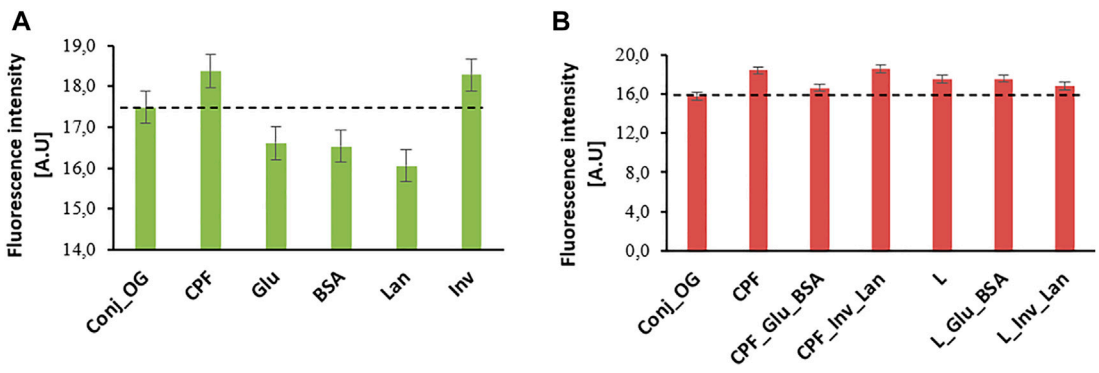

FIGURE 8 | Fluorescence response of the system in the presence of 0.1 ppm of different analytes in tap water. **(A)** Selectivity of the system for individual tests and **(B)** matrix effect of some mixes. The dotted line indicates the baseline (CD–AChE conjugate with GO). *n* = 6 independent experiments.

effect, whereas carbamates, such as methomyl, form a less stable complex that can easily split from AChE through spontaneous hydrolysis (decarbamylation) (Colovic et al., 2013). On the other hand, Invetrina® shows a signal comparable with CPF detection. Pyrethroid substances are esters with an alcohol and acid moiety. The acid moiety usually contains a dimethylcyclopropane ring with a variable radical, and within the alcohol moiety, most of the synthetic pyrethroids contain aromatic rings and sometimes a cyano group (Sogorb and Vilanova, 2002). Even though pyrethroids are not known as AChE inhibitory compounds, aromatic and other chemical groups may cause interference in the measure leading to a false positive. This could be inferred also from the matrix effect assay (**Figure 8B**) when the CPF detection in the presence of Invetrina and lanate did not show interference because the affinity of the AChE for CPF is more specific and stronger than the random chemical groups interacting with the cypermethrin.

Regarding the matrix effect, groups of the same substances used for the selectivity test were evaluated at 0.025 ppm in the presence of 0.01 ppm of CPF and Lorsban® (L) in tap water. **Figure 8B** shows that the detection of CPF is affected by common organic molecules, such as glucose (Glu) and BSA, but not by the presence of non-organophosphate pesticides. Instead, detection of Lorsban® is not affected by glucose or BSA and is slightly affected by the other pesticides. As expected, the coadjutants in the commercial formulation of Lorsban protect the active principle against other molecules that could degrade it or make a shielding effect. In the case of CPF, the active principle is bare and exposed to the environmental effect of other molecules. Both in selectivity and matrix effect, the different ions present in tap water seem to not influence the performance of the system, fostering its field application.

CONCLUSION

In summary, a sensitive biosensor based on acetylcholinesterase and carbon dot–graphene oxide quenching test was developed for the detection of analytical-grade chlorpyrifos. Furthermore, the system shows good results for the detection of a commercial formula called Lorsban®, based on chlorpyrifos. This should be highlighted because in the fumigation of crops, commercial formulations, such as Lorsban®, are used instead of pure chlorpyrifos. To the best of our knowledge, a few studies report on commercial pesticide detection. The conjugation between acetylcholinesterase enzyme and carbon dots was deeply characterized, and powerful insights about the chemical group's interactions as well as size and stability were obtained. The results suggested that the biosensor works through a FRET principle, using graphene oxide (GO) as a universal quenching agent. In this way, the system exhibited a good exponential relationship of the fluorescence recovery and the pesticide concentration, obtaining an ultralow LOD of 0.14 and 2.05 ppb for chlorpyrifos and Lorsban®, respectively. These results agree with the state of the art reporting the high sensibility of the fluorescence systems, especially with the incorporation of nanomaterials in turning-on mode. The biosensor showed good results in tap water and the presence of possible coexisting substances, indicating the potential of field implementation. However, the specificity, sensibility, and repeatability of the biosensor, in general, is still a major limitation for their implementation into point-of-care systems. In the present work, the repeatability of the data must be improved, considering the inherent challenges of the enzymatic-based systems, and detecting commercial pesticide formulations in field samples. In this sense, strategies like the use of single-stranded nucleic acids (aptamers), instead of enzymes, and the immobilization of the biomolecules could be applied for future studies. Nevertheless, and given its simplicity, this study paves the way for the implementation of portable systems based on nanotechnology for the detection of environmental pollutants.

DATA AVAILABILITY STATEMENT

The raw data supporting the conclusion of this article will be made available by the authors, without undue reservation.

AUTHOR CONTRIBUTIONS

Devised and directed the project JC and GP; designed the experiments and conceptualized the paper MG, KB, and JA; performed the conjugation assays MG; characterized the conjugate and data analysis MG, KB, and JA; conducted the detection assays and data analysis MG, KB, and JA.; wrote the manuscript in consultation, MG, KB, JA, JC, and GP. All authors discussed the results and commented on the manuscript. All authors have read and agreed to the published version of the manuscript.

FUNDING

This work was funded by the Ministry of Science, Technology, and Innovation of the Colombian government (code 111571451059, contract number FP44842-147-2016; code 133380764415, contract number CT- 800-2018).

ACKNOWLEDGMENTS

The authors would like to thank the Ministry of Science, Technology, and Innovation of the Colombian government for financing the projects "Redes de biosensores aplicados a la detección de contaminantes tóxicos en fuentes naturales que abastecen a las plantas de potabilización" (code 111571451059, contract number FP44842-147-2016) and "Desarrollo de un inmunosensor basado en Carbon Dots para la detección de *tuberculosis*" (code 133380764415, contract number CT- 800-2018). The authors thank the Ministry of Science, Technology, and Innovation of the Colombian government for the scholarship for the doctoral studies of MG (Grant number 785 of 2017).

REFERENCES

Abdul, S., Nor, R., and Zobir, M. (2019). *Synthesis, Technology and Applications of Carbon Nanomaterials*. Oxford: Elsevier.

Alvandi, N., Assariha, S., Esfandiari, N., and Jafari, R. (2021). Off-on Sensor Based on Concentration-dependent Multicolor Fluorescent Carbon Dots for Detecting Pesticides. *Nano-Structures & Nano-Objects* 26, 100706. doi:10.1016/j.nanoso.2021.100706

Arvand, M., and Mirroshandel, A. A. (2019). An Efficient Fluorescence Resonance Energy Transfer System from Quantum Dots to Graphene Oxide Nano Sheets: Application in a Photoluminescence Aptasensing Probe for the Sensitive Detection of Diazinon. *Food Chem.* 280 (November), 115–122. doi:10.1016/j.foodchem.2018.12.069

Ashrafi Tafreshi, F., Fatahi, Z., Ghasemi, S. F., Taherian, A., and Esfandiari, N. (2020). Ultrasensitive Fluorescent Detection of Pesticides in Real Sample by Using green Carbon Dots. *PLoS One* 15 (3), e0230646–17. doi:10.1371/journal.pone.0230646

Bai, Y., Xu, T., and Zhang, X. (2020). Graphene-based Biosensors for Detection of Biomarkers. *Micromachines* 11 (1). doi:10.3390/mi11010060

Bao, J., Huang, T., Wang, Z., Yang, H., Geng, X., Xu, G., et al. (2019). 3D Graphene/copper Oxide Nano-Flowers Based Acetylcholinesterase Biosensor for Sensitive Detection of Organophosphate Pesticides. *Sensors Actuators, B Chem.* 279 (May), 95–101. doi:10.1016/j.snb.2018.09.118

Barrientos, K., Gaviria, M. I., Arango, J. P., Londoño, M. E., and Jaramillo, M. (2021). Synthesis, Characterization and Ecotoxicity Evaluation of Biochar-Derived Carbon Dots from Spruce Tree, Purple Moor-Grass and African Oil Palm. *Processes* 9, 1095. doi:10.3390/pr9071095

Berger, A. R., and Schaumburg, H. H. (2005). Human Toxic Neuropathy Caused by Industrial Agents. *Peripher. Neuropathy* 2, 2505–2525. doi:10.1016/b978-0-7216-9491-7.50115-0

Betancur, J., Morales, D. F., Peñuela, G. A., and Cano, J. B. (2018). Detección de Clorpirifos en Leche usando un Biosensor Enzimático Amperométrico basado en Acetilcolinesterasa. *Inf. Tecnol.* 29 (6), 113–122. doi:10.4067/s0718-07642018000600113

Blotnick-Rubin, E., and Anglister, L. (2018). Fine Localization of Acetylcholinesterase in the Synaptic Cleft of the Vertebrate Neuromuscular Junction. *Front. Mol. Neurosci.* 11, 123. doi:10.3389/fnmol.2018.00123

Bourne, Y., Grassi, J., Bougis, P. E., and Marchot, P. (1999). Conformational Flexibility of the Acetylcholinesterase Tetramer Suggested by X-ray Crystallography. *J. Biol. Chem.* 274 (43), 30370–30376. doi:10.1074/jbc.274.43.30370

Cacciotti, I., Pallotto, F., Scognamiglio, V., Moscone, D., and Arduini, F. (2020). Reusable Optical Multi-Plate Sensing System for Pesticide Detection by Using Electrospun Membranes as Smart Support for Acetylcholinesterase Immobilisation. *Mater. Sci. Eng. C* 111, 110744. doi:10.1016/j.msec.2020.110744

Campuzano, S., Yáñez-Sedeño, P., and Pingarrón, J. M. (2019). Carbon Dots and Graphene Quantum Dots in Electrochemical Biosensing. *Nanomaterials* 9 (4), 1–18. doi:10.3390/nano9040634

Catalina Rodríguez, D., Carvajal, S., and Peñuela, G. (2013). Effect of Chlorpyrifos on the Inhibition of the Enzyme Acetylcholinesterase by Cross-Linking in Water-Supply Samples and Milk from Dairy Cattle. *Talanta* 111, 1–7. doi:10.1016/j.talanta.2013.03.036

Chang, H., Tang, L., Wang, Y., Jiang, J., and Li, J. (2010). Graphene Fluorescence Resonance Energy Transfer Aptasensor for the Thrombin Detection. *Anal. Chem.* 82 (6), 2341–2346. doi:10.1021/ac9025384

Chen, S., and Cashman, J. R. (2013). *Organophosphate Exposure: Detection and Remediation*. 1st ed., 7. Amsterdam: Elsevier B.V.

Chen, Y., Qin, X., Yuan, C., Shi, R., and Wang, Y. (2020). Double Responsive Analysis of Carbaryl Pesticide Based on Carbon Quantum Dots and Au Nanoparticles. *Dyes Pigm.* 181 (April), 108529. doi:10.1016/j.dyepig.2020.108529

Cheng, X., Cen, Y., Xu, G., Wei, F., Shi, M., Xu, X., et al. (2018). Aptamer Based Fluorometric Determination of ATP by Exploiting the FRET between Carbon Dots and Graphene Oxide. *Mikrochim Acta* 185 (2), 144–148. doi:10.1007/s00604-018-2683-z

Colovic, M. B., Krstic, D. Z., Lazarevic-Pasti, T. D., Bondzic, A. M., and Vasic, V. M. (2013). Acetylcholinesterase Inhibitors: Pharmacology and Toxicology. *Cn* 11 (3), 315–335. doi:10.2174/1570159x11311030006

da Silva, M. K. L., Vanzela, H. C., Defavari, L. M., and Cesarino, I. (2018). Determination of Carbamate Pesticide in Food Using a Biosensor Based on Reduced Graphene Oxide and Acetylcholinesterase Enzyme. *Sensors Actuators B: Chem.* 277 (August), 555–561. doi:10.1016/j.snb.2018.09.051

Das, G. P., Jamil, K., and Rahman, M. F. (2006). Effect of Four Organophosphorus Compounds on Human Blood Acetylcholinesterase: *In Vitro* Studies. *Toxicol. Mech. Methods* 16 (8), 455–459. doi:10.1080/15376520600719281

Ding, Y., Ling, J., Wang, H., Zou, J., Wang, K., Xiao, X., et al. (2015). Fluorescent Detection of Mucin 1 Protein Based on Aptamer Functionalized Biocompatible Carbon Dots and Graphene Oxide. *Anal. Methods* 7 (18), 7792–7798. doi:10.1039/c5ay01680k

Dobbertin, A., Hrabovska, A., Dembele, K., Camp, S., Taylor, P., Krejci, E., et al. (2009). Targeting of Acetylcholinesterase in Neurons *In Vivo*: A Dual Processing Function for the Proline-Rich Membrane Anchor Subunit and the Attachment Domain on the Catalytic Subunit. *J. Neurosci.* 29 (14), 4519–4530. doi:10.1523/jneurosci.3863-08.2009

Dong, J., Zhao, H., Qiao, F., Liu, P., Wang, X., and Ai, S. (2013). Quantum Dot Immobilized Acetylcholinesterase for the Determination of Organophosphate Pesticides Using Graphene-Chitosan Nanocomposite Modified Electrode. *Anal. Methods* 5, 2866. doi:10.1039/c3ay26599d

Ellman, G. L., Courtney, K. D., Andres, V., and Featherstone, R. M. (1961). A New and Rapid Colorimetric Determination of Acetylcholinesterase Activity. *Biochem. Pharmacol.* 7, 88–95. doi:10.1016/0006-2952(61)90145-9

FAO (2018). *Pesticides Indicators*. FAOSTAT. Available at: http://www.fao.org/faostat/en/#data/EP/visualize (Accessed March 17, 2021).

Gaviria-Arroyave, M. I., Cano, J. B., and Peñuela, G. A. (2020). Nanomaterial-based Fluorescent Biosensors for Monitoring Environmental Pollutants: A Critical Review. *Talanta Open* 2 (June), 100006. doi:10.1016/j.talo.2020.100006

He, S., Song, B., Li, D., Zhu, C., Qi, W., Wen, Y., et al. (2010). A Graphene Nanoprobe for Rapid, Sensitive, and Multicolor Fluorescent DNA Analysis. *Adv. Funct. Mater.* 20 (3), 453–459. doi:10.1002/adfm.200901639

Huang, S., Yao, J., Chu, X., Liu, Y., Xiao, Q., and Zhang, Y. (2019). One-Step Facile Synthesis of Nitrogen-Doped Carbon Dots: A Ratiometric Fluorescent Probe for Evaluation of Acetylcholinesterase Activity and Detection of Organophosphorus Pesticides in Tap Water and Food. *J. Agric. Food Chem.* 67 (40), 11244–11255. doi:10.1021/acs.jafc.9b03624

Işık, M. (2020). High Stability of Immobilized Acetylcholinesterase on Chitosan Beads. *ChemistrySelect* 5 (15), 4623–4627. doi:10.1002/slct.202000559

Ismail, B. S., and Ngan, C. K. (2005). Dissipation of Chlorothalonil, Chlorpyrifos, and Profenofos in a Malaysian Agricultural Soil: A Comparison between the Field experiment and Simulation by the PERSIST Model. *J. Environ. Sci. Health B* 40 (2), 341–353. doi:10.1081/pfc-200045560

Jokanović, M. (2018). Neurotoxic Effects of Organophosphorus Pesticides and Possible Association with Neurodegenerative Diseases in Man: A Review. *Toxicology* 410 (September), 125–131. doi:10.1016/j.tox.2018.09.009

Kaur, N., and Prabhakar, N. (2017). Current Scenario in Organophosphates Detection Using Electrochemical Biosensors. *Trac Trends Anal. Chem.* 92, 62–85. doi:10.1016/j.trac.2017.04.012

Khoris, I. M., Ganganboina, A. B., Suzuki, T., and Park, E. Y. (2021). Self-assembled Chromogen-Loaded Polymeric Cocoon for Respiratory Virus Detection. *Nanoscale* 13 (1), 388–396. doi:10.1039/d0nr06893d

King, A. M., and Aaron, C. K. (2015). Organophosphate and Carbamate Poisoning. *Emerg. Med. Clin. North America* 33 (1), 133–151. doi:10.1016/j.emc.2014.09.010

Kumar, T. H. V., and Sundramoorthy, A. K. (2019). Electrochemical Biosensor for Methyl Parathion Based on Single-Walled Carbon Nanotube/glutaraldehyde Crosslinked Acetylcholinesterase-Wrapped Bovine Serum Albumin Nanocomposites. *Analytica Chim. Acta* 1074, 131–141. doi:10.1016/j.aca.2019.05.011

Lee, J., Kim, J., Kim, S., and Min, D.-H. (2020). Biosensors Based on Graphene Oxide and its Biomedical Application. *Adv. Drug Deliv. Rev.* 105 (January), 275–287. doi:10.1016/j.addr.2016.06.001

Li, H., Su, D., Gao, H., Yan, X., Kong, D., Jin, R., et al. (2020). Design of Red Emissive Carbon Dots: Robust Performance for Analytical Applications in Pesticide Monitoring. *Anal. Chem.* 92 (4), 3198–3205. doi:10.1021/acs.analchem.9b04917

Li, M., Zhou, X., Guo, S., and Wu, N. (2013). Detection of lead (II) with a "Turn-On" Fluorescent Biosensor Based on Energy Transfer from CdSe/ZnS Quantum

Dots to Graphene Oxide. *Biosens. Bioelectron.* 43 (1), 69–74. doi:10.1016/j.bios.2012.11.039

Liu, M. L., Chen, B. B., Li, C. M., and Huang, C. Z. (2019). Carbon Dots: Synthesis, Formation Mechanism, Fluorescence Origin and Sensing Applications. *Green. Chem.* 21 (3), 449–471. doi:10.1039/c8gc02736f

Luo, D., Zhou, T., Tao, Y., Feng, Y., Shen, X., and Mei, S. (2016). Exposure to Organochlorine Pesticides and Non-hodgkin Lymphoma: A Meta-Analysis of Observational Studies. *Sci. Rep.* 6 (1), 25768. doi:10.1038/srep25768

Mao, H., Yan, Y., Hao, N., Liu, Q., Qian, J., Chen, S., et al. (2017). Dual Signal Amplification Coupling Dual Inhibition Effect for Fabricating Photoelectrochemical Chlorpyrifos Biosensor. *Sensors Actuators B: Chem.* 238, 239–248. doi:10.1016/j.snb.2016.07.072

Mishra, I. P., Sabat, G., and Mohanty, B. K. (2015). Phytotoxicity of Profenofos 50% EC (Curacron 50 EC) to Vigna Radiata,L. Seedlings: II. Studies on Biochemical Parameters. *Int. J. Appl. Sci. Biotechnol.* 3 (1), 101–105. doi:10.3126/ijasbt.v3i1.12063

Mostafalou, S., and Abdollahi, M. (2018). The Link of Organophosphorus Pesticides with Neurodegenerative and Neurodevelopmental Diseases Based on Evidence and Mechanisms. *Toxicology* 409 (July), 44–52. doi:10.1016/j.tox.2018.07.014

Nagabooshanam, S., Roy, S., Mathur, A., Mukherjee, I., Krishnamurthy, S., and Bharadwaj, L. M. (2019). Electrochemical Micro Analytical Device Interfaced with Portable Potentiostat for Rapid Detection of Chlorpyrifos Using Acetylcholinesterase Conjugated Metal Organic Framework Using Internet of Things. *Sci. Rep.* 9 (1), 19862–19869. doi:10.1038/s41598-019-56510-y

Neema, P. M., Tomy, A. M., and Cyriac, J. (2020). Chemical Sensor Platforms Based on Fluorescence Resonance Energy Transfer (FRET) and 2D Materials. *Trac Trends Anal. Chem.* 124, 115797. doi:10.1016/j.trac.2019.115797

Pang, Y.-P., Singh, S. K., Gao, Y., Lassiter, T. L., Mishra, R. K., Zhu, K. Y., et al. (2009). Selective and Irreversible Inhibitors of Aphid Acetylcholinesterases: Steps toward Human-Safe Insecticides. *PLoS One* 4 (2), e4349. doi:10.1371/journal.pone.0004349

Pirsaheb, M., Mohammadi, S., and Salimi, A. (2019). Current Advances of Carbon Dots Based Biosensors for Tumor Marker Detection, Cancer Cells Analysis and Bioimaging. *Trac Trends Anal. Chem.* 115, 83–99. doi:10.1016/j.trac.2019.04.003

Ramírez, J. A., and Lacasaña, M. (2001). Pesticides: Classification, Uses, Toxicological Aspects and Exposure Assesment. *Arch. Prev. Riesgos Labo* 4 (2), 67–75.

Ramnani, P., Saucedo, N. M., and Mulchandani, A. (2016). Carbon Nanomaterial-Based Electrochemical Biosensors for Label-free Sensing of Environmental Pollutants. *Chemosphere* 143, 85–98. doi:10.1016/j.chemosphere.2015.04.063

Ratner, M. H., and Jabre, J. F. (2016). "Neurobehavioral Toxicology," in *Module in Neuroscience and Biobehavioral Psychology* (Amsterdam: Elsevier), 423–439.

Raves, M. L., Giles, K., Schrag, J. D., Schmid, M. F., Phillips, G. N., Chiu, W., et al. (1998). "Quaternary Structure of Tetrameric Acetylcholinesterase," in *Structure and Function of Cholinesterases and Related Proteins* (Boston, MA: Springer), 351–356. doi:10.1007/978-1-4899-1540-5_97

Reshma, R., Gupta, B., Sharma, R., and Ghosh, K. K. (2019). Facile and Visual Detection of Acetylcholinesterase Inhibitors by Carbon Quantum Dots. *New J. Chem.* 43 (25), 9924–9933. doi:10.1039/c9nj02347j

Sánchez-Santed, F., Colomina, M. T., and Herrero Hernández, E. (2016). Organophosphate Pesticide Exposure and Neurodegeneration. *Cortex* 74, 417–426. doi:10.1016/j.cortex.2015.10.003

Shamagsumova, R., Rogov, A., Shurpik, D., Stoikov, I., and Evtugyn, G. (2021). Acetylcholinesterase Biosensor Based on Reduced Graphene Oxide – Carbon Black Composite for Determination of Reversible Inhibitors. *Electroanalysis* 33, 1–11. doi:10.1002/elan.202100385

Sharma, S. K., Micic, M., Li, S., Hoar, B., Paudyal, S., Zahran, E. M., et al. (2019). Conjugation of Carbon Dots with β-Galactosidase Enzyme: Surface Chemistry and Use in Biosensing. *Molecules* 24 (18), 3275. doi:10.3390/molecules24183275

Shukla, A. K., and Iravani, S. (2019). *Green Synthesis, Characterization and Applications of Nanoparticles*. Amsterdam: Elsevier.

Sidhu, G. K., Singh, S., Kumar, V., Dhanjal, D. S., Datta, S., and Singh, J. (2019). Toxicity, Monitoring and Biodegradation of Organophosphate Pesticides: A Review. *Crit. Rev. Environ. Sci. Tech.* 49 (13), 1135–1187. doi:10.1080/10643389.2019.1565554

Sogorb, M. A., and Vilanova, E. (2002). Enzymes Involved in the Detoxification of Organophosphorus, Carbamate and Pyrethroid Insecticides through Hydrolysis. *Toxicol. Lett.* 128 (1–3), 215–228. doi:10.1016/s0378-4274(01)00543-4

Song, J., and Zhang, J. (2019). Self-illumination of Carbon Dots by Bioluminescence Resonance Energy Transfer. *Sci. Rep.* 9, 13796–13797. doi:10.1038/s41598-019-50242-9

Suner, S. S., Sahiner, M., Ayyala, R. S., Bhethanabotla, V. R., and Sahiner, N. (2021). Versatile Fluorescent Carbon Dots from Citric Acid and Cysteine with Antimicrobial, Anti-biofilm, Antioxidant, and AChE Enzyme Inhibition Capabilities. *J. Fluoresc.* 31 (6), 1705–1717. doi:10.1007/s10895-021-02798-x

Suo, Z., Liu, X., Hou, X., Liu, Y., Lu, J., Xing, F., et al. (2020). Ratiometric Assays for Acetylcholinesterase Activity and Organo-Phosphorous Pesticide Based on Superior Carbon Quantum Dots and BLGF-Protected Gold Nanoclusters FRET Process. *ChemistrySelect* 5 (29), 9254–9260. doi:10.1002/slct.202002042

Talari, F. F., Bozorg, A., Faridbod, F., and Vossoughi, M. (2021). A Novel Sensitive Aptamer-Based Nanosensor Using rGQDs and MWCNTs for Rapid Detection of Diazinon Pesticide. *J. Environ. Chem. Eng.* 9 (1), 104878. doi:10.1016/j.jece.2020.104878

Ubaid ur Rahman, H., Asghar, W., Nazir, W., Sandhu, M. A., Ahmed, A., and Khalid, N. (2020). A Comprehensive Review on Chlorpyrifos Toxicity with Special Reference to Endocrine Disruption: Evidence of Mechanisms, Exposures and Mitigation Strategies. *Sci. Total Environ.* 755, 142649. doi:10.1016/j.scitotenv.2020.142649

Vinotha Alex, A., and Mukherjee, A. (2021). Review of Recent Developments (2018–2020) on Acetylcholinesterase Inhibition Based Biosensors for Organophosphorus Pesticides Detection. *Microchem. J.* 161 (November), 105779. doi:10.1016/j.microc.2020.105779

Wei, J., Cao, J., Hu, H., Yang, Q., Yang, F., Wan, J., et al. (2017). Sensitive and Selective Detection of Oxo-form Organophosphorus Pesticides Based on CdSe/ZnS Quantum Dots. *Molecules* 22 (9), 1–11. doi:10.3390/molecules22091421

Wu, X., Wang, P., Hou, S., Wu, P., and Xue, J. (2019). Fluorescence Sensor for Facile and Visual Detection of Organophosphorus Pesticides Using AIE Fluorogens-SiO2-MnO2 sandwich Nanocomposites. *Talanta* 198 (January), 8–14. doi:10.1016/j.talanta.2019.01.082

Xu, X., Cen, Y., Xu, G., Wei, F., Shi, M., and Hu, Q. (2019). A Ratiometric Fluorescence Probe Based on Carbon Dots for Discriminative and Highly Sensitive Detection of Acetylcholinesterase and Butyrylcholinesterase in Human Whole Blood. *Biosens. Bioelectron.* 131 (February), 232–236. doi:10.1016/j.bios.2019.02.031

Zhang, J., Hu, H., and Yang, L. (2021). Ultra-highly Sensitive and Stable Acetylcholinesterase Biosensor Based on TiO2-NRs and rGO. *Microchemical J.* 168 (March), 106435. doi:10.1016/j.microc.2021.106435

Zheng, X. T., Ananthanarayanan, A., Luo, K. Q., and Chen, P. (2015). Glowing Graphene Quantum Dots and Carbon Dots: Properties, Syntheses, and Biological Applications. *Small* 11 (14), 1620–1636. doi:10.1002/smll.201402648

Zhou, J., Ai, R., Weng, J., Li, L., Zhou, C., Ma, A., et al. (2020). A "On-Off-On" Fluorescence Aptasensor Using Carbon Quantum Dots and Graphene Oxide for Ultrasensitive Detection of the Major Shellfish Allergen Arginine Kinase. *Microchemical J.* 158, 105171. doi:10.1016/j.microc.2020.105171

Conflict of Interest: The authors declare that the research was conducted in the absence of any commercial or financial relationships that could be construed as a potential conflict of interest.

Publisher's Note: All claims expressed in this article are solely those of the authors and do not necessarily represent those of their affiliated organizations, or those of the publisher, the editors, and the reviewers. Any product that may be evaluated in this article, or claim that may be made by its manufacturer, is not guaranteed or endorsed by the publisher.